Adapting a Frequency-Domain Optical Equalizer without Regressor Access

A.G. Klein
Dept. of Elec. & Cmptr. Engr.
WPI, Worcester, MA 01609
contact email: klein@wpi.edu

B.M. Evans, C.R. Johnson, Jr.
School of Elec. & Computer Engr.
Cornell University, Ithaca, NY 14850

G. Collins, M.G. Larimore, J.C. Harp, J.R. Treichler
Applied Signal Technology
Sunnyvale, California 94086

***Abstract*—We consider the development of adaptive algorithms for use with an optical equalizer. The task of adaptively equalizing an optical signal has two notable challenges not present in traditional electrical equalization: 1) Access to a finite window of past equalizer inputs (i.e. the regressor) is impractical, and 2) The difficulty in building a true optical tapped delay line leads to implementations which are expected to have peculiar parameterizations as well as constraints on how the "taps" can be adjusted. We present a regressor-free algorithm suitable for adapting a prototype frequency-domain optical equalizer. In addition, we present trained and blind versions of the algorithm, and conclude with simulations demonstrating algorithm performance.**

I. Introduction

Just as the push for faster and faster data rates is ceaseless, so too are the implementation challenges in building wireless hardware to support such rates. We have seen the same technological evolution time and time again in wireless communications [1]: in the quest for higher data rates, a new technology is considered for use in an environment which inevitably introduces channel dispersion; dispersion compensation algorithms and techniques are developed, often long before the necessary hardware exists; finally, as the hardware matures, these techniques are reduced to practice and evolved through several cycles of implementation improvements.

Free-space optical communication is one such technology which is increasingly being given attention as a viable means of enabling communication at tens or hundreds of gigabits per second. As expected, one of the key issues confronting terrestrial free space optical communications is channel dispersion, an impairment which only becomes more severe with increasing data rates. A study was conducted 15 years ago [2] which determined that optical filtering had seen little attention largely because of the fact that hardware did not yet exist or was not mature enough to build useful adaptive optical tapped delay lines or other optical filtering structures. Looking again at the literature and the products currently available on the market indicates that, 15 years later, progress is just beginning in this area. Recent advances in optical hardware and MEMS technology have enabled the possibility of building prototype optical tapped delay lines suitable for use with adaptive algorithms (see [3] and references therein). Such optical tapped delay lines are typically mixed electrical-optical devices, with the filtering performed in the optical domain and the tap adjustment performed electronically. When a photodiode converts an optical signal into an electrical signal, the nonlinear nature of photodiode effectively discards the phase information; thus, performing equalization on a converted electrical signal is not a viable option. Consequently, adaptive optical equalization exhibits several practical limitations that preclude direct application of traditional equalization algorithms to optical communication systems, and raises two notable challenges that, taken together, make for a novel problem that has not been addressed in traditional electrical equalization. First, access to a finite window of past equalizer inputs (i.e. the regressor) is not likely to be possible. The only hope for measuring the high speed optical input to the equalizer would be by splitting the signal before the equalizer, and passing it through a photodiode. Even if the particular implementation did permit this, however, the photodiode would not preserve necessary phase information and is therefore of limited use. Secondly, the difficulty in building a true optical tapped delay line leads to implementations which are expected to have peculiar (and possibly not perfectly characterized) parameterizations, as well as constraints on how the "taps" can be adjusted. While most electrical equalizers are implemented as pure tapped delay lines, early MEMS-based optical equalizers are not expected to be able to accurately represent an ideal tapped delay line.

We thus consider the development of adaptive algorithms for use with hardware implementations that exhibit these two characteristics: lack of regressor information, and a non-standard parameterization of the taps, which may additionally have an implementation-induced reachability constraint. While the algorithms we develop are general enough for any application that exhibits these characteristics, the motivation for such algorithms is the emergence of a prototype optical equalizer, called the Essex Optical Equalizer (EOE) [4]. The EOE is essentially a frequency-domain optical filter that permits phase-only adjustments to the frequency bins. In the next section, we will describe the basic operation of the optical equalizer, as well as a mathematical model for its operation. Next, we will present a regressor-free algorithm for adaptation of the equalizer taps, which is in the class of localized random-search algorithms. We will consider an algorithm that requires training data, as well as one which can be operated in a

This work was supported in part by Applied Signal Technology and the National Science Foundation.

blind mode. Finally, we demonstrate the performance of the algorithms with numerical simulations.

II. The Essex Optical Equalizer

A. Physical Operation of the EOE

We first describe the operation of the prototype EOE, which is the target hardware platform for our regressor-free algorithm. The EOE, shown in Fig. 1, is essentially a frequency domain equalizer which permits phase-only adjustments to the frequency bins. The optical input signal enters the device, and the hyperfine channelizer uses a set of prisms to perform an approximate instantaneous Fourier transform, splitting the signal into $N = 128$ discrete channels or frequency bins. The

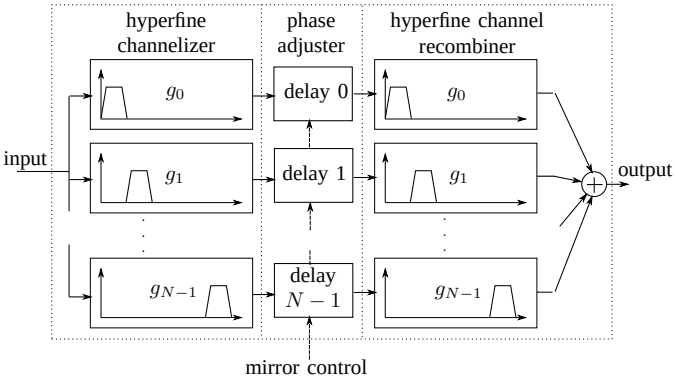

Fig. 1. Essex Optical Equalizer Block Diagram

phase of each of the frequency bins is then altered with a series of adjustable MEMS mirrors, and the signal is subsequently passed back through a hyperfine channel recombiner which acts as an approximate inverse Fourier transform (and is precisely the channelizer operated in reverse). We note that the signal path through the EOE is purely in the optical domain, though the control signal which adjusts the MEMS mirror positions is an electrical signal.

As the MEMS mirror positions are adjustable, they allow control of the path length through the EOE, and hence they permit control of the phase of the signal in each frequency bin. The mirrors do not, however, permit relative amplitude control, so the EOE cannot be controlled to have an arbitrary frequency response. Furthermore, the EOE is fully parameterized by the N mirror positions $\boldsymbol{d} \in [0, d_{max}]^N$ which have hard limits on how far they can be physically adjusted, given by d_{max}. Thus, the EOE has an implementation-induced constraint on the range of possible mirror positions, and consequently a constraint on the range of possible frequency responses it can assume.

B. System Model for the EOE

We now develop an equivalent digital representation of the EOE shown in Fig. 1, inspired by the transmultiplexer structure in [5][6, pp. 164-172]. While the hyperfine channelizer splits the signal into N frequency bins, the precise impulse response (or *point spread function*) is not likely to be a pure Fourier transform of the input. Therefore, we model the channelizer as a cosine modulated filter bank, operating over the frequencies $[-B, B]$ and based on a prototype filter $g(t)$, where each component filter is given by

$$g_i(t) = g(t)\cos\left(\frac{2\pi B(i+1/2)t}{N}\right), \text{ for } i = 0, \ldots, N-1.$$

It is expected that the prototype filter $g(t)$ has bandwidth approximately equal to B/N, as shown in the example in Fig. 2 for $N = 8$. Note that if $g(t)$ has bandwidth less than

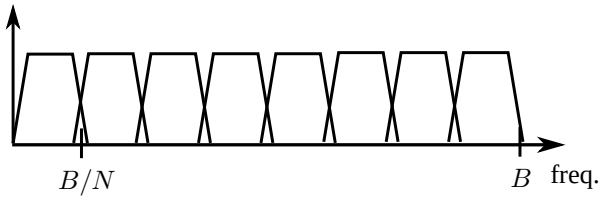

Fig. 2. Example Frequency Channelization for $N = 8$

B/N, then some frequencies will not pass through the device; on the other hand, if the bandwidth of $g(t)$ is larger than B/N, then adjacent frequency bins will be overlapping. The MEMS mirrors each introduce a displacement d_i along the ith path, which corresponds to a round-trip temporal delay of $2d_i/c$ where c is the speed of light. After including the effect of the channel recombiner, the continuous time impulse response of the EOE is given by

$$f(t) = \sum_{i=0}^{N-1} g_i(t - 2d_i/c) \star g_i(t).$$

Now let

$$\begin{aligned} f_i(t) &\triangleq g_i(t) \star g_i(t) \\ &= \int_{-\infty}^{\infty} g(\tau)g(t-\tau)\cos\left(\frac{2\pi B(i+1/2)\tau}{N}\right) \\ &\quad \cdot \cos\left(\frac{2\pi B(i+1/2)(t-\tau)}{N}\right) d\tau \end{aligned} \quad (1)$$

and let T_s denote the sample period used to develop the digital equivalent representation, where it is assumed that T_s is sufficiently small to satisfy the Nyquist criterion. Thus, the sampled impulse response of the EOE is given by

$$f[n] = \sum_{i=0}^{N-1} f_i(nT_s - 2d_i/c). \quad (2)$$

Then, for a given operating bandwidth B, number of channels N, and prototype filter $g(t)$ which characterizes the hyperfine frequency channelizer, equations (1) and (2) allow us to compute the equivalent T_s-spaced impulse response $h[n]$ for the EOE, parameterized by the mirror positions $\boldsymbol{d}$.

C. End-to-end System Model

The end-to-end system model is shown in Fig. 3, where optical signals are denoted by solid lines and electrical signals are denoted by dashed lines. We assume that on-off keying (OOK) is used at the transmitter, and that symbols are sent

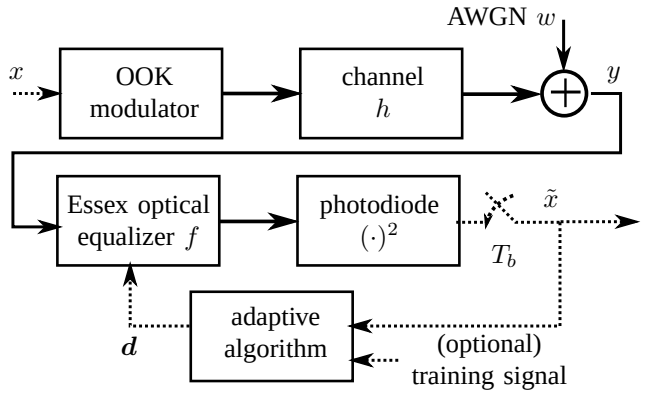

Fig. 3. End to End System Model

over a dispersive channel with additive white Gaussian noise. Note that the channel is assumed to be unknown to both the transmitter and receiver. The optical received signal is processed by the EOE, and then passed into a square-law photodiode which converts the signal from an optical signal into an electrical signal. The adaptive algorithm which we will design then adjusts the mirror positions of the equalizer, and only has access to the electrical baud-rate photodiode output and possibly a training sequence. We assume that all electrical signals are baud-rate signals having sample period T_b, whereas the optical signals are represented by a higher-rate digital signal with underlying sample period T_s, where $T_s P = T_b$ for some oversampling factor P which for simplicity is assumed to be a (strictly positive) integer. Let $x_{op}[n]$ denote the optical transmitted signal so that $x_{op}[n]$ is simply a rate $1/T_s$ upsampled version of $x[n]$. Similarly, let $\tilde{x}_{op}[n]$ denote the rate $1/T_s$ photodiode output before downsampling. The received signal (i.e. the signal comprising the regressor) can then be expressed as

$$y[n] \quad = \quad x_{op}[n] \star h[n] + w[n] \tag{3}$$

where $h[n]$ is the T_s-spaced channel impulse response, $w[n]$ is the AWGN. Together with (3), then, the input-output relation of the system is

$$\tilde{x}_{op}[n] \quad = \quad (y[n] \star f[n])^2 \tag{4}$$

where $f[n]$ is the EOE impulse response given by (2). Under ideal operation, then, the baud-rate photodiode output $\tilde{x}[n]$ is approximately equal to a delayed version of the source $x[n]$. We are now ready to consider the development of a regressor-free algorithm for adapting the N phases or mirror positions $\boldsymbol{d}$ of the EOE.

III. A Regressor-free Adaptive Algorithm

As we have mentioned, the equalizer input $y[n]$ is an optical signal, and is consequently not available for use by a candidate adaptive algorithm. As shown in Table I, we can roughly place equalization algorithms into one of four categories, depending on the availability of training and regressor information. The case where regressor information is available — regardless of the availability of training data — has received much attention in the literature, and is by now a fairly classical problem with a variety of well-known [7] algorithms including LMS, RLS, CMA, etc. The case where no regressor information is available has seen much less attention; unless some particular structure of the system can be exploited, it seems that random search techniques are the only means of performing equalization.

	presence of training	absence of training
presence of regressor	LMS, RLS, etc.	CMA, etc.
absence of regressor	random search	random search

TABLE I
Categories of Equalization Algorithms

Our goal is the development of an adaptive equalization algorithm which has *no* regressor information and *no* training data. Since the design of a regressor-free algorithm is quite formidable, we will begin by first considering an algorithm that has training data available, and then later proceed to the case without training data.

A. Trained version of algorithm

Again, since regressor information is not available to the adaptive equalization algorithm, we consider using random search algorithms. Let $\mathcal{D} = [0, d_{max}]^N$ denote the set of admissible equalizer taps. The goal is to find a set of equalizer taps or mirror positions $\boldsymbol{d} \in \mathcal{D}$ so that the optical equalizer sufficiently mitigates the distortion introduced by the channel $h[n]$. We first choose some cost function, $J(\boldsymbol{d})$ that we seek to minimize. This cost might be an estimate of the mean-squared error at the photodiode output, it could be the cluster variance, or it could perhaps be some quantity based on the Q-factor. The (regressor-free) random search algorithm proceeds as follows, which is sometimes called *search by natural selection* [8] or *localized random search* [9]:

1) Pick some initial $\boldsymbol{d}[0] \in \mathcal{D}$.
2) Calculate current cost $J(\boldsymbol{d}[n])$.
3) Pick a random additive adjustment $\Delta\boldsymbol{d}[n]$ for the filter taps, where $E[\Delta\boldsymbol{d}[n]] = \boldsymbol{0}$ and $\mathrm{cov}(\Delta\boldsymbol{d}[n]) = \sigma_d^2 \boldsymbol{I}$. Verify that $\boldsymbol{d}[n] + \Delta\boldsymbol{d}[n] \in \mathcal{D}$. If not, pick another random $\Delta\boldsymbol{d}[n]$.
4) Calculate cost of $J(\boldsymbol{d}[n] + \Delta\boldsymbol{d}[n])$.
5) Is $J(\boldsymbol{d}[n] + \Delta\boldsymbol{d}[n]) < J(\boldsymbol{d}[n])$?
   If yes, update taps via $\boldsymbol{d}[n+1] = \boldsymbol{d}[n] + \Delta\boldsymbol{d}[n]$.
   If no, don't update, so $\boldsymbol{d}[n+1] = \boldsymbol{d}[n]$.
6) Increment n. Goto step 2.

We note that the corresponding tap update equation can be written succinctly as

$$\boldsymbol{d}[n+1] \quad = \quad \boldsymbol{d}[n] + \frac{\Delta\boldsymbol{d}[n]}{2} \cdot [1 + \mathrm{sgn}\left(J(\boldsymbol{d}[n]) - J(\boldsymbol{d}[n] + \Delta\boldsymbol{d}[n])\right)]$$

and indeed this is regressor-free so long as the chosen cost $J(\boldsymbol{d})$ does not depend on the equalizer input $y[n]$. Algorithm convergence rate and stability are controlled by the variance σ_d^2 of the random move direction. The convergence rate and

misadjustment of a similar, though unconstrained algorithm were investigated for updating a standard tapped delay line in [8]. In [8], it was shown that for a fixed rate of adaptation, the classical LMS algorithm has a misadjustment proportional to the number of taps, while random search algorithms have a misadjustment proportional to the square of the number of taps. Similarly, for a fixed level of misadjustment that can be tolerated, the LMS convergence time is proportional to the number of taps, while the random search algorithm convergence time is proportional to the square of the number of taps. Thus, there is a significant penalty to be paid when the regressor is unavailable.

We note that, in generating the random choice of adjustment direction $\Delta \boldsymbol{d}[n]$, not all values are admissible as some random mirror settings will be beyond the maximum allowable mirror displacement. Consequently, while the random search proceeds, we only accept adjustments where the mirror settings $\boldsymbol{d}$ are within the allowable range.

As a cost function for use when training data is available, we use an M-sample estimate of the MSE of the photodiode output, formed as

$$J_{trained}(\boldsymbol{d}) \quad = \quad \frac{1}{M} \sum_{k=0}^{M-1} |\tilde{x}[n-k] - x[n-k-\Delta]|^2 \quad (5)$$

where Δ is a designer-selected symbol delay through the channel/equalizer combination.

B. Algorithm for use in the absence of training data

Blind equalization algorithms (i.e. those which do not require training data) *do* rely on knowledge of the statistics of the source, and they generally try to make the equalizer output statistics "look like" the source statistics. In a traditional electrical system that uses, say, BPSK modulation, it is well-known that blind equalization algorithms have two inherent ambiguities: a delay ambiguity, and a sign ambiguity. Such delay and sign ambiguities are generally not a problem, however, and we can expect these ambiguities to be present in this problem, as well. The use of OOK symbols in conjunction with the square-law photodiode, however, raises another ambiguity in this blind equalization problem, as we now show.

We consider a source that consists of OOK symbols assuming value 0 or 1 with equal probability. Clearly, any single-spike impulse response (in the absence of noise) will generate a signal at the photodiode output with identical statistics. In addition, however, the baud-spaced length-2 impulse response $q(z^{-1}) = 1 - z^{-1}$ will also generate a signal with this distribution at the photodiode output. In fact, the combination of the impulse response $1 - z^{-1}$ (or delayed, sign-flipped versions) together with the square-law photodiode essentially performs a form of differential encoding of the OOK symbols, again resulting in a sequence of symbols that are also 0 or 1 with equal probability. This is not catastrophic, however, as the original source sequence can still be recovered through differential decoding. Consequently, while the desired combined channel/equalizer response is a single-spike, we must also be willing to accept the baud-spaced impulse response $[+1, -1]$ as a solution of any candidate blind algorithm.

For our blind version of our algorithm, we employ a form of decision direction. We assume that the OOK symbols assume value 0 or 1 with equal probability, and we consider use of a simple slicer that makes decisions at the output of the square-law photodiode, defined as

$$\mathcal{Q}(\tilde{x}[n]) \quad = \quad \begin{cases} 1 & \text{for } \tilde{x}[n] > \gamma \\ 0 & \text{for } \tilde{x}[n] \leq \gamma \end{cases}$$

where the maximum likelihood (ML) decision threshold is chosen to be $\gamma = (1/2)^2 = 1/4$. We can then use the same random search algorithm outlined above, but with a decision-directed cost function given by:

$$J_{dd}(\boldsymbol{\theta}) \quad = \quad \frac{1}{N} \sum_{k=0}^{N-1} |\tilde{x}[n-k] - \hat{x}[n-k]|^2 \quad (6)$$

where $\hat{x}[n] = \mathcal{Q}(\tilde{x}[n])$ is the output of the decision device device at time n.

IV. Numerical Examples

A. Example with Training

For the numerical simulations we conduct here, we choose $N = 128$ frequency bins, a bandwidth of $B = 15$ GHz, a baud rate of $1/T_b = 10$ GHz, a sample period of $T_s = 25$ ps (resulting in an oversampling factor of 4), and we fix the SNR at 20 dB. While a parallel EOE experimentation effort is ongoing, we do not yet have a precise characterization of the point spread function of the EOE, and hence the exact prototype filter $g(t)$ is not known. Thus, we choose $g(t)$ to be the square-root raised cosine pulse with rolloff $\beta = 0.3$, so that $f(t)$ is the raised-cosine pulse and the frequency bins are partially overlapping. For the algorithm parameters, we form the MSE estimate by averaging a window of size $M = 20$ symbols, and the random update for each d_i is uniformly distributed between ± 0.001 where $d_{max} = 0.02$. We consider performance over the T_s-spaced channel with impulse response given by

$$\boldsymbol{h} \quad = \quad [0.0108, -0.0179, 0.0299, -0.0498, 0.0830, -0.1383, \\ 0.2306, -0.3843, 0.6404, 0.5994]^\top$$

and we initialize the mirrors to the middle of their extent, so $d_i = 0.01$ for all i.

The results from one sample run of the trained algorithm are shown in Fig. 4, where we see that the algorithm in this case converged (near) to the MMSE impulse response after approximately $4 \cdot 10^6$ symbols at 20 dB SNR. We note that the algorithm occasionally updates the equalizer taps to a setting with worse MSE from one iteration to the next; this is because the algorithm minimizes the sample estimate of the MSE, and not the true MSE. In addition, we note that the MMSE solution shown in Fig. 4 is the MMSE over all possible impulse responses $f[n]$; since the EOE cannot reach arbitrary impulse responses, this MMSE is a lower bound on the minimum MSE attainable by the EOE. An exhaustive

numerical search would have to be performed to find the true MMSE for the EOE since the MSE is not a simple function of the mirror settings $\boldsymbol{d}$. Finally, we note that the convergence time can vary widely, and we have only shown one sample run here. We will explore the issue of average convergence time further in the next section.

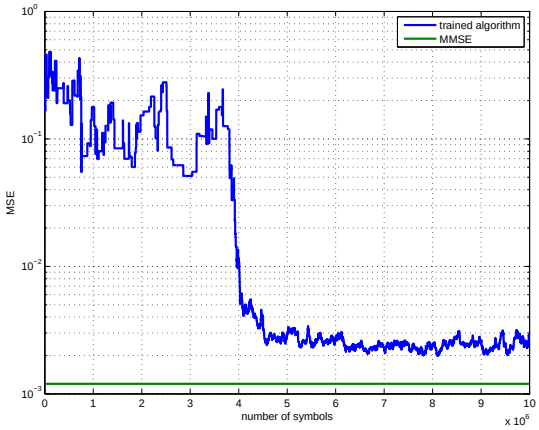

Fig. 4. Example of convergence of trained algorithm on EOE

B. Decision-directed Convergence Time

As mention previously, it was shown in [8] that for a fixed level of misadjustment, random search algorithm convergence time is proportional to the square of the number of taps. Here, we attempt to demonstrate experimentally that a similar behavior exists in our decision-directed adaptive algorithm. We now vary the number of mirror settings (or taps) N, and consider the convergence time by averaging over 1,000 random initializations of the N mirror settings d_i when a unity channel is used, i.e. $h[n] = \delta[n]$. The choice of a unity channel guarantees that the equalizer admits a solution for any amount of mirror settings N. Though the 1,000 random initializations are typically closed-eye situations, the decision-directed random search algorithm eventually finds a solution given enough time.

We use the same parameters as in Section IV-A above, but we replace the training data with decision-directed data and we vary the number of mirror settings N. At each value of $N \in \{2, 4, 8, 16, 32\}$, we calculate the number of symbols the algorithm requires to reach an MSE of -10 dB. Since the decision-directed algorithm can converge to any delay, as well as the effective combined response $1 - z^{-1}$ (as discussed in Section III-C), we calculate the MSE at each iteration by first finding the MSE between the current equalizer setting and all acceptable solutions (i.e. delayed single-spike impulse responses, as well as $1 - z^{-1}$), and then we chose the minimum.

The results are shown in Fig. 5, where indeed the convergence time generally obeys a quadratic behavior. In addition, we have plotted the best quadratic fit to this curve, corresponding to the function $371.3N^2$. The large amount of simulation time required for values of N beyond 32 is prohibitively long. However, extrapolating to $N = 128$ suggests that an estimate for the average number of symbols required for convergence is approximately $6 \cdot 10^6$. While this is admittedly a large number of symbols, this is the price to pay when regressor information is unavailable. Furthermore, with optical data rates in the tens of gigahertz, the amount of real time to convergence would be on the order of a millisecond.

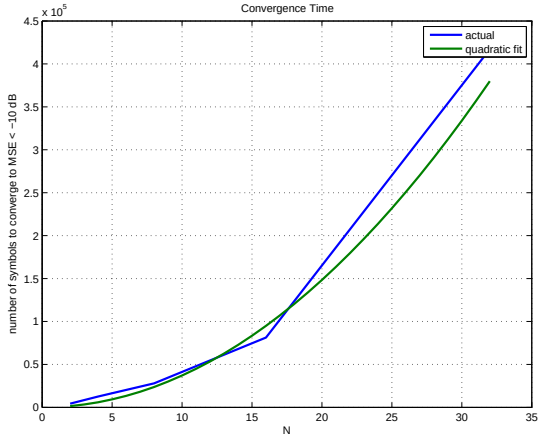

Fig. 5. Convergence time of decision-directed algorithm on EOE

V. Conclusion

We have proposed a regressor-free adaptive algorithm suitable for use with emerging optical equalizers. In particular, we have focussed on adapting a prototype Essex optical equalizer which permits phase-only adjustment of the frequency bins. Through simulation, we have seen that the algorithm does indeed find an acceptable equalizer tap setting – both in trained and decision-directed modes – and succeeds in reducing the channel dispersion even in cases where the eye is initially closed. While the algorithm can often take very many symbols to converge, we note that 10^7 symbols is a fairly small amount of time at 10 GHz data rates – on the order of 1 millisecond.

References

[1] J. Treichler, M. Larimore, and J. Harp, "Practical blind demodulators for high-order QAM signals," *Proc. IEEE*, vol. 86, pp. 1907–1926, Oct. 1998.

[2] R. Bitmead, C. R. Johnson, Jr., and C. Pollock, "Optical adaptive signal processing: An appraisal," *International Journal of Adaptive Control and Signal Processing*, vol. 5, pp. 87–92, 1991.

[3] M. Bohn, W. Rosenkranz, and P. Krummrich, "Adaptive distortion compensation with integrated optical finite impulse response filters in high bitrate optical communication systems," *IEEE J. Sel. Topics Quantum Electron.*, vol. 10, pp. 273–280, Mar. 2004.

[4] T. M. Turpin *et al.*, "Optical tapped delay line," U.S. Patent 6 608 721, Aug. 19, 2003.

[5] G. Copeland, "Transmultiplexers used as adaptive frequency sampling filters," in *Proc. IEEE Intl. Conf. on Acoustics, Speech, and Signal Processing (ICASSP'82)*, May 1982, pp. 319–322.

[6] E. Ferrara, "Frequency-domain adaptive filtering," in *Adaptive Filters*, C. Cowan and P. Grant, Eds. Englewood Cliffs, NJ: Prentice-Hall, 1985.

[7] S. Haykin, *Adaptive Filter Theory*, 4th ed. Upper Saddle River, N.J.: Prentice Hall, 2001.

[8] B. Widrow and J. McCool, "A comparison of adaptive algorithms based on the methods of steepest descent and random search," *IEEE Trans. Antennas Propag.*, vol. 24, pp. 615–637, Sep. 1976.

[9] F. J. Solis and R. J.-B. Wets, "Minimization by random search techniques," *Mathematics of Operations Research*, vol. 6, pp. 19–30, Feb. 1981.